hv photonics

IMPACT FACTOR 2.1

CITESCORE 2.6

Article

Enhancement of Charging Performance of Micromaser Quantum Battery via Classical Driving Field and Optical Parametric Amplifier

Jia Zuo, Sumei Huang, Li Deng and Aixi Chen

Special Issue

Nonlinear Optics and Optical Parametric Oscillators: From Fundamentals to Cutting-Edge Research

Edited by

Dr. Wange Song

MDPI

https://doi.org/10.3390/photonics12030177

photonics

MDPI

Article

Enhancement of Charging Performance of Micromaser Quantum Battery via Classical Driving Field and Optical Parametric Amplifier

Jia Zuo [1], Sumei Huang [1], Li Deng [2] and Aixi Chen [2,*]

[1] Zhejiang Key Laboratory of Quantum State Control and Optical Field Manipulation, Department of Physics, Zhejiang Sci-Tech University, Hangzhou 310018, China; 202220102092@mails.zstu.edu.cn (J.Z.); sumei@zstu.edu.cn (S.H.)
[2] School of Science, Zhejiang Sci-Tech University, Hangzhou 310018, China; lideng75@zstu.edu.cn
* Correspondence: aixichen@zstu.edu.cn

Abstract: In this paper, we propose a scheme where the charging performance of micromaser quantum batteries can be improved. Our physical system includes a quantized cavity field interacting with a series of identical two-level atoms one by one. In order to improve the performance of the battery, two methods are introduced: one is using a controlling field to drive atoms, and the other is placing OPA crystals in the cavity. Under these different methods, we discuss the influence of different parameters on battery capacity. Finally, combining the two methods for charging yields better results than using either of them alone. These protocols are found to be stable and robust, and most of the stored energy in the quantum batteries can be extracted for work. Our scheme has a potential applications in quantum energy storage devices.

Keywords: quantum batteries; micromasers; classical driving field; optical parametric amplifier

Received: 13 January 2025
Revised: 15 February 2025
Accepted: 19 February 2025
Published: 21 February 2025

Citation: Zuo, J.; Huang, S.; Deng, L.; Chen, A. Enhancement of Charging Performance of Micromaser Quantum Battery via Classical Driving Field and Optical Parametric Amplifier. *Photonics* **2025**, *12*, 177. https://doi.org/10.3390/photonics12030177

1. Introduction

In recent years, the trend towards the miniaturization of technology and devices operating at the nanoscale has led to the expansion of traditional thermodynamic concepts such as work and heat to explain quantum mechanical effects, resulting in the emergence of the field of quantum thermodynamics. Researchers have conducted a series of studies on quantum thermodynamic devices with different functions, and quantum batteries are a major research hotspot. Unlike the concepts of lithium batteries and lead–acid batteries that we usually refer to, quantum batteries can be composed of various substances, such as ions, neutral atoms, photons, or organic polymer materials, as long as these materials can form quantum entanglement systems. Simply put, a quantum battery [1–3] is a quantum system that provides temporary energy storage, storing energy provided by external sources and making it available for use by other devices. Alicki and Fannes [4] were the first to work on this topic, and subsequent research has expanded in several different directions. A series of quantum battery models have been proposed, including simple models such as two-level system quantum batteries or resonant quantum batteries [5–9], as well as many multibody quantum battery models [10–20], including Sachdev–Ye–Kitaev batteries [21], the Tavis–Cummings quantum battery [22,23], the Dicke quantum battery [16,24], random quantum batteries [25], spin-chain quantum batteries [10,12,26,27], and so on. Most research focuses on the energy stored in quantum batteries, the energy available for operation, charging power, and other properties. Sachdev–Ye–Kitaev batteries utilize the collective

effects of quantum many-body systems to achieve energy. This research contributes to a deep understanding of complex phenomena such as quantum entanglement. However, there are challenges in applying its results and theories to the real world. The Tavis–Cummings quantum battery utilizes multiple two-level atoms (qubits) to couple and interact with a single-mode optical field in the cavity, which can improve the efficiency of energy storage and transmission. However, the model's ability to describe multi-mode and complex optical field environments is limited. The Dicke quantum battery is a system composed of multiple two-level atoms (qubits), which helps to gain a deeper understanding of the physical properties and working principles of multi-qubit systems in quantum batteries. However, approximate conditions lead to certain deviations between theoretical calculations and actual situations. The principle of Random quantum batteries is based on the randomness and fluctuation characteristics in quantum systems. It can flexibly optimize the performance of quantum batteries. However, it places high demands on experimental techniques. Spin chain quantum batteries are composed of a series of coupled spin particles (qubits), and are beneficial for achieving higher energy storage capacity and more powerful functionality. However, the interactions between spins in spin chains are very complex, and the strength and direction of these interactions are difficult to precisely control and adjust in actual quantum battery systems, which may lead to unpredictable and difficult-to-optimize performance of quantum batteries.

As energy storage devices that utilize quantum effects, the core advantage of quantum batteries lies in their ability to achieve efficient energy storage and transfer. This technology utilizes quantum correlation and entanglement properties to break the limitations of traditional batteries in energy storage and transmission efficiency, providing new possibilities for future energy storage technologies [28,29]. With the advancement of technology and the continuous pursuit of energy efficiency, the application of quantum batteries has gradually become a hot research topic. Especially in the face of increasing energy demand, the development of quantum batteries is particularly important, as it has the potential to reconstruct thermodynamic and dynamic laws at the microscale through the characteristics of quantum systems, and achieve new principle energy storage and supply devices with a smaller size, stronger charging power, higher charging capacity, and larger extractable work [30,31].

Despite facing many challenges in the development and application of quantum batteries, such as aging and environmentally induced decoherence, scientists have made some progress. In recent years, collision models [19,32–35] have become a hot research topic. Using quantum resonators or large spins as models, batteries are charged through sequential interactions (collisions) with a stream of qubits. When the qubits are prepared in some coherent state, they exhibit stronger performance than their classical counterparts compared to non-coherent charging. In previous studies, it has been demonstrated that a micromaser [36–41] charged through coherent qubits can be considered an excellent model for quantum batteries. In a micromaser, the flow of a two-level system (qubit) interacts sequentially with the electromagnetic field in the cavity, simulating a quantum harmonic oscillator. In fact, this system has recently been proposed as an excellent model for quantum batteries and can be described using the famous Jaynes–Cummings model [42,43]. In this article, we will discuss methods to improve battery charging performance based on existing theoretical foundations.

Quantum batteries rely on quantum states to store and transfer energy, but quantum states are highly susceptible to environmental noise such as fluctuations [44] and electromagnetic interference [45], leading to decoherence [46] and the loss of their unique quantum properties, resulting in the loss of quantum information. This affects the accuracy of energy storage and operation, making it difficult to effectively store and transfer energy, thereby

affecting battery performance. To maintain the stability of quantum states, it is necessary to develop effective anti-interference technologies. The existing energy system is based on classical physics principles, while quantum batteries are based on quantum mechanics, and their energy extraction and conversion mechanisms are different. Moreover, existing energy systems may not be able to directly utilize the energy output from quantum batteries, and efficient storage and extraction of energy from quantum states remains a challenge. In order to achieve efficient energy transfer, further research is needed. Research on quantum batteries is an important component of the development of quantum technology. Solving the technical challenges faced by quantum batteries will drive theoretical and experimental breakthroughs in these fields, promote the development of related quantum technologies such as quantum computers and quantum communications, and open up a new era of quantum technology applications. With the continuous growth of global energy demand, traditional energy is facing depletion and environmental pollution problems, and there is an urgent need for new and efficient energy storage technologies. Quantum batteries theoretically have higher energy storage density and charge–discharge efficiency, meeting future energy demands.

In this article, we explore methods to improve the charging performance of micromaser quantum batteries. First, we use a controlling field to drive atoms; in other words, we apply a driving field to the qubits in the system, which occurs before interacting with the battery, to explore the maximum charging capacity [47] and extractable energy [13,48,49] of the quantum battery. Then, we place optical parametric amplifier (OPA) [50–52] crystals in the cavity to study its performance and investigate the influence of different parameters on battery energy. Finally, on the basis of these two methods, we attempt to combine them and observe whether the combined approach has advantages over the individual approach. In the end, we conclude that they all can improve battery performance to a certain extent.

2. Model

As shown in Figure 1, the quantum battery is composed of a quantized electromagnetic field (EM) inside the cavity, which is regarded as a quantum harmonic oscillator. This quantum battery is initially prepared in the ground state $|0\rangle$. The charging process involves a series of identical two-level atoms (qubits) continuously interacting with the quantum battery to achieve the effect of charging the battery. The initial state of each two-level atom is

$$\rho_q = q|g\rangle\langle g| + (1-q)|e\rangle\langle e| + c\sqrt{q(1-q)}(|g\rangle\langle e| + |e\rangle\langle g|), \tag{1}$$

where $q \in [0,1]$ controls the degrees of population inversion. When $q = 0$, the qubit is in an excited state; when $q = 1$, the qubit is in the ground state; and when $q \in (0,1)$, it is in a superposition state of the ground state and the excited state. $c \in [0,1]$ controls the degrees of population coherence. Qubits are in an incoherent state when $c = 0$, a coherent state when $c = 1$, and an incompletely coherent state when $c \neq 1$. The interaction between a qubit and the cavity field is described by the Hamiltonian

$$\begin{aligned} H &= H_0 + H_1 \\ H_0 &= \omega_a a^\dagger a + \omega_q \sigma_+ \sigma_- \\ H_1 &= g\left(a\sigma_+ + a^\dagger \sigma_- + a^\dagger \sigma_+ + a\sigma_-\right) \end{aligned}, \tag{2}$$

where ω_a and ω_q are the frequencies of the field and the qubit, respectively; $a^\dagger$ is the creation operator of the harmonic oscillator and a is the annihilation operator; and σ_+ and σ_- are the rising and lowering operators of qubits, respectively. g represents the coupling coefficient between the field and the qubit. We usually take $\hbar = 1$, and we also consider the

case of resonance between the field and qubit, which means that the frequencies of the field and qubit are equal and taken as ω.

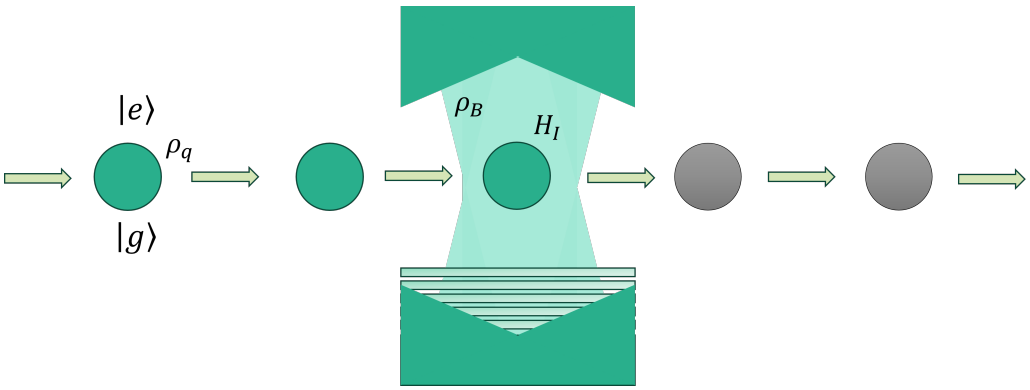

Figure 1. A diagram of a micromaser quantum battery. The qubits on the left indicate that they are in a superposition state of ground and excited states at the time of entry. The middle shows that the qubits enter the cavity and interact with the electromagnetic field. The qubits on the right indicate a decrease in their interaction energy with the EM field.

It is convenient to describe the dynamic behavior in the interaction picture; therefore, in the interaction picture, the Hamiltonian of the system evolution is simplified as

$$H_I = g\left(a\sigma_+ + a^\dagger\sigma_- + e^{i2\omega t}a^\dagger\sigma_+ + e^{-i2\omega t}a\sigma_-\right), \tag{3}$$

We usually refer to the first two terms in the above equation as rotating terms, and the last two terms as counter-rotating terms. From this, we can derive the time evolution operator as

$$U_I(\tau) \equiv \mathcal{T}\exp\left\{-i\int_0^\tau H_I(t)dt\right\}, \tag{4}$$

where $\mathcal{T}$ is the time-ordering operator and τ is the interaction time between a single qubit input and a harmonic oscillator. For the sake of simplicity and effectiveness, we fix $\tau = 1$.

As is well known, a time-dependent Hamiltonian means that the energy of a system is not a constant, but a function that varies over time. This makes the dynamic behavior of the system complex and difficult to analyze. Therefore, omitting the counter-rotating terms of the above equation can greatly simplify our calculation process. We all know that when $g/\omega \ll 1$, the counter-rotating terms can be omitted, which is the familiar JC model. However, in the charging process of quantum batteries, weak coupling can lead to slow charging, which is not what we want. In order to improve the charging speed of quantum batteries, the ultrastrong coupling regime of $0.1 < \frac{g}{\omega} < 1$ is worth considering. We will use the method introduced in Ref. [43], which shows that by simultaneously modulating the frequency of the qubit and the field, the counter-rotating terms can be neglected, and the resulting dynamics are described by the Jaynes–Cummings (JC) unitary operator. In Refs. [40,43], it has been proven that the time evolution operator can be expressed as

$$U_I(g) = e^{-ig(a\sigma_+ + a^\dagger\sigma_-)}, \tag{5}$$

and the coherence parameter c can be set to be real by applying a rotation along the z axis, which does not alter the time evolution operator $U_I(g)$. At this point, the Hamiltonian is $H_I' = g(a\sigma_+ + a^\dagger\sigma_-)$.

In the battery charging process, as depicted in Figure 1, the battery is initially in a pure state $|0\rangle$, which means that the charging process of the battery is initialized by the cavity in its ground state $\rho_B = |0\rangle\langle 0|$. With $\rho_B(k)$ denoting the battery state after having interacted

with k qubits, $k = 0, \ldots, n$, we use $\rho(k) = \rho_B(k) \otimes \rho_q$ to represent the state of the system. The time evolution can be written as

$$\rho_B(k+1) = \mathrm{Tr}_q[U_I(g)\rho(k)U_I^\dagger(g)], \tag{6}$$

where Tr_q is the trace over qubit degrees of freedom.

3. Figures of Merit

The above equation represents the iterative relationship of the charging process; we can calculate the relevant performance of quantum batteries based on this iterative relationship, such as the battery's ability to store energy, charging power, work extraction, etc.

The energy stored [5,6,9,53] in the quantum battery after k interactions with a qubit is represented by $E(k) = \mathrm{Tr}(H_B\rho_B(k))$, where $H_B = \omega a^\dagger a$ is the battery Hamiltonian and the trace is taken over battery degrees of freedom. When we know the energy of a battery, its performance can be quantified according to the charging power [2,54–57]. We define the charging power of a battery as $P = \frac{E(k)}{k\tau}$; here, τ is the time of a single interaction between the qubit and the battery, and we take it as 1, that is, $P = \frac{E(k)}{k}$.

For batteries, we hope that the energy charged can be effectively utilized. If the energy can be fully utilized, we require the purity of the fully charged battery to be 1, and the expression for purity is $\mathcal{P}(k) \equiv \mathrm{Tr}(\rho_B^2)$.

The indicators for measuring the performance of quantum batteries also include ergotropy [58], which is the maximum energy that can be released during an ideal discharge process. It refers to the ability of quantum batteries to generate useful work, and its mathematical expression is

$$\mathcal{E}_B(k) = E(k) - \min_U \mathrm{tr}[H_B U \rho_B U^\dagger] \ . \tag{7}$$

By diagonalizing H_B and ρ_B separately, we can obtain

$$\begin{array}{c} H_B = \sum_n e_n |e_n\rangle\langle e_n| \\ \rho_B(k) = \sum_n r_n(k) |r_n(k)\rangle\langle r_n(k)| \end{array} . \tag{8}$$

The eigenvalues of ρ_B are arranged in descending order as $r_0 \gg r_1 \gg \cdots$, and the eigenvalues of H_B are arranged in ascending order as $e_0 \ll e_1 \ll \cdots$. The right-hand side of the formula can be simplified as

$$\min_U \mathrm{tr}[H_B U \rho_B U^\dagger] = \sum_n r_n e_n \ . \tag{9}$$

Thus, this formula can be transformed into

$$\mathcal{E}_B(k) = E(k) - \sum_n r_n e_n. \tag{10}$$

It is easy to obtain $\mathcal{E}_B(k) \ll E(k)$ from the above equation, so we can define the efficiency $R(k)$ as the percentage of ergotropy $\mathcal{E}_B(k)$ to $E(k)$, that is, $R(k) = \frac{E_B(k)}{E(k)}$, describing the release efficiency of useful energy in quantum batteries.

4. Classical Driving Field

In Ref. [40], the researchers demonstrated numerically that a micromaser can quickly charge to achieve an almost steady state. And they showed that for a micromaser, the almost steady states mentioned above are approximately pure; therefore, in principle, almost all energy can be reversibly extracted. This is a very surprising feature.

On the model of the original system, we want to find a suitable method to improve the performance of the battery. We try to add a driving field before the qubits interact with

the cavity to drive these two-level atoms, as shown in Figure 2. The Hamiltonian of the added driving field is

$$H_d = f(e^{-i\omega_d t}\sigma_+ + e^{i\omega_d t}\sigma_-), \tag{11}$$

here, f is the driving field strength, and the frequency of the driving field is represented by ω_d.

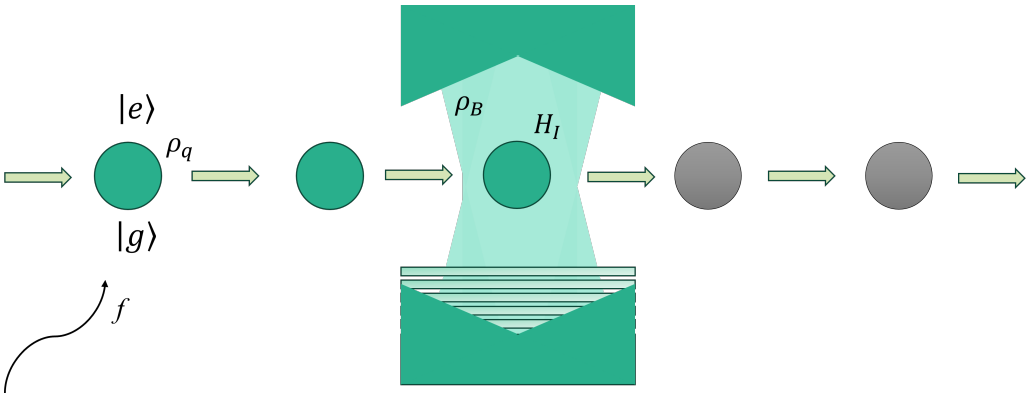

Figure 2. A diagram of a micromaser quantum battery operating via the classical driving field. Before the qubits enter the cavity, we add a classical driving field to drive them. The strength of this driving field is represented by f.

When the driving field frequency is equal to the transition frequency of a two-level atom, a resonance phenomenon occurs. This greatly improves the energy exchange efficiency between qubits and cavities, reduces losses during energy transfer, and enhances the charging speed and efficiency of quantum batteries. Appropriate classical field driving can create an equivalent shielding environment around the qubit, changing the coupling mode between the qubit and the external environment, and reducing the impact of external noise and interference on the qubit. In this way, qubits can better maintain their quantum properties during the interaction with the cavity, reduce energy loss and information loss, and help improve the overall performance of quantum batteries. Our discussion is based on the assumption that the frequency of the driving field is equal to the transition frequency of the qubit. After a unitary transformation, the above equation can be transformed into $H_d' = f(\sigma_+ + \sigma_-)$. In the frame rotation, the total Hamiltonian of the system, $H_D = H_I' + H_d'$, can be written as

$$H_D = g(a\sigma_+ + a^\dagger\sigma_-) + f(\sigma_+ + \sigma_-), \tag{12}$$

In the framework of quantum electrodynamics, when a classical driving field acts on a qubit, it will couple with the qubit. The driving field can be represented as an oscillating electromagnetic field that interacts with the electric dipole moment of a qubit, and a term describing this interaction is introduced into the Hamiltonian. This interaction can cause changes in the energy level structure of qubits. When the frequency of the classical driving field and the energy level transition frequency of the qubit satisfy the resonance condition, the qubit will undergo periodic transitions between the two energy levels. When the classical driving field acts on the qubit, if the driving field frequency is equal to or very close to the energy level transition frequency of the qubit, that is, the absolute value of the difference between the two is small enough, the transition probability of the qubit between different energy levels will greatly increase [59–65].

After obtaining the Hamiltonian of the system, we can study the performance of quantum batteries. The impact of driving on the primary battery is what we need to explore.

For comparison, we choose the same parameters as in Ref. [40], $q = 0.25$, $c = 1$. The initial state of a qubit is the superposition of the ground state and excited state. As discussed in Ref. [40], the particle number inversion parameter q is inversely proportional to the steady-state energy. A larger value of q will reduce the steady-state energy. When q approaches 0.5, the charging efficiency is very low. At this time, although the steady state is stable, the energy is extremely low. The influence of parameter q on the steady-state energy of the battery is explained from both theoretical and practical perspectives. The purity of a battery has an approximately linear functional relationship with c, where the higher c, the higher the purity of the battery. When $c < 1$, the steady-state energy significantly increases, and the ergotropy is positively affected, but at the cost of a shorter lifetime of the steady state. A larger c value means a longer lifetime of the steady state, but at the cost of lower energy and ergotropy. The calculations in this article are very complicated. For convenience, we use QUTIP [66] to calculate and analyze the data, and all operations are completed using QUTIP.

Firstly, let us observe the energy storage characteristics of the battery. The following figure shows our numerical results. Representing the energy of the quantum battery as a function of the number of interactions.

In Figure 3, we can easily see that the green color in the picture represents the numerical results of not adding the classical driving field, and the purple color represents the numerical results after adding the classical driving field. It can be clearly observed that the system can also quickly stabilize after adding the classical driving field.

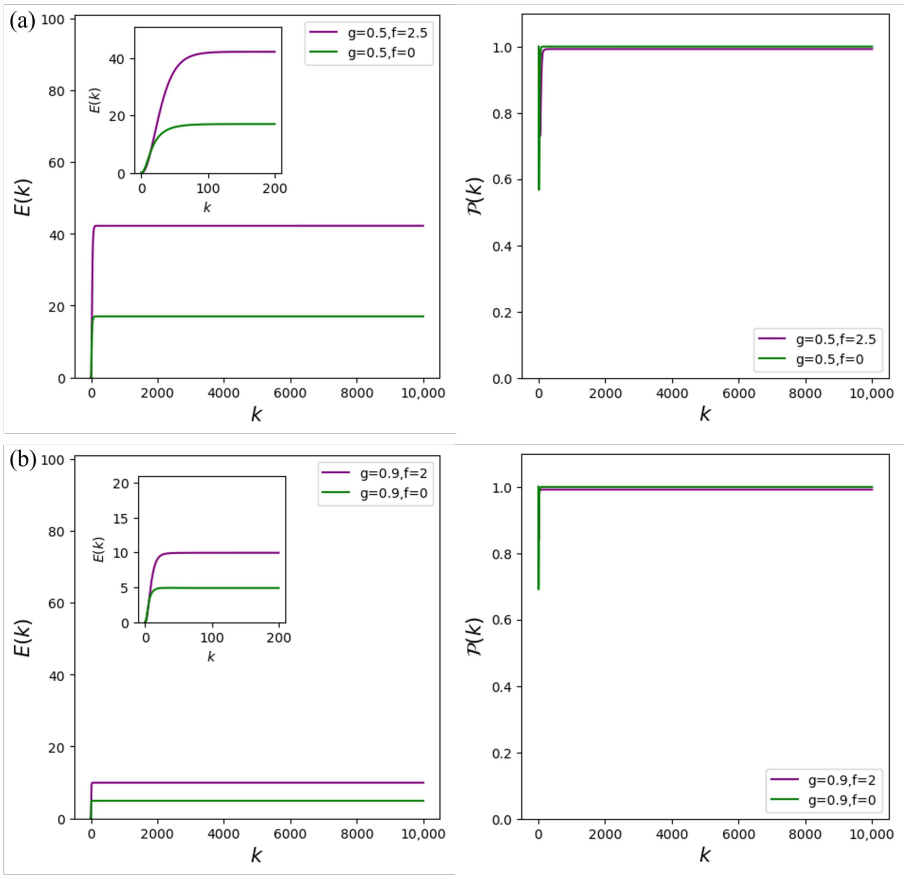

Figure 3. The performance of the micromaser quantum battery. The **left** panel represents the energy stored and the **right** panel represents purity; they are computed for $q = 0.25$, $c = 1$, and we intercept the Hilbert space $N = 100$. For comparison purposes, (**a**) $g = 0.5$ and $f = 0$, 2.5 in the panel. The values on the **left** panel are approximately 42.24 and 17.02 from top to bottom. (**b**) $g = 0.9$ and $f = 0, 2$ in the panel. The values on the **left** panel are approximately 9.95 and 4.90 from top to bottom.

As shown in Figure 3, at $g = 0.5$, the system stabilizes after 100 interactions and remains stable after 10^4 interactions, and the energy after the battery stabilizes is significantly higher than before; at $g = 0.9$, the system remains stable after 25 cycles and remains stable even after 10^4 cycles. Although the value of k reaching a steady state increases, it is worth noting that the energy of the battery significantly increases after stabilization. And we can observe from the above figure that the final state of the battery is close to a pure state, indicating that the energy stored in the battery can be almost completely utilized.

This is a good result, but does this characteristic still exist when we take different driving strength values? This is the question we need to explore. From this, we can conclude that adding the driving field can to some extent increase the energy storage of the battery.

Then, we investigate the relationship between driving strength and battery energy. In the previous text, we only found a good value among many values to improve energy storage while the battery is basically in a pure state. To further discuss the impact of adding the driving field on battery charging, we calculated the steady-state energy and ergotropy of quantum batteries under different driving intensities, as shown in the following figure.

From the graph, we can clearly see the process of the battery's energy $E(k)$ changing as the driving strength f increases. When $g = 0.5$, it can be seen that the energy $E(k)$ gradually increases with f until f approaches 3.7. When $g = 0.9$, it can be seen that the energy $E(k)$ gradually increases with f until f approaches 7.

In Figure 4, we plot the energy of the battery $E(k)$ as a solid purple line and the extractable energy (ergotropy) $\mathcal{E}_B(k)$ as a solid blue line, which clearly shows the variation in both with the driving strength f. We have found an interesting phenomenon whereby before the energy stored in the battery reaches its maximum value, the images of energy $E(k)$ and extractable energy (ergotropy) $\mathcal{E}_B(k)$ overlap, which means that the energy stored in the battery can be almost completely used, which is an ideal result. Afterwards, the amount of energy that can be effectively released from the energy charged into the battery decreases.

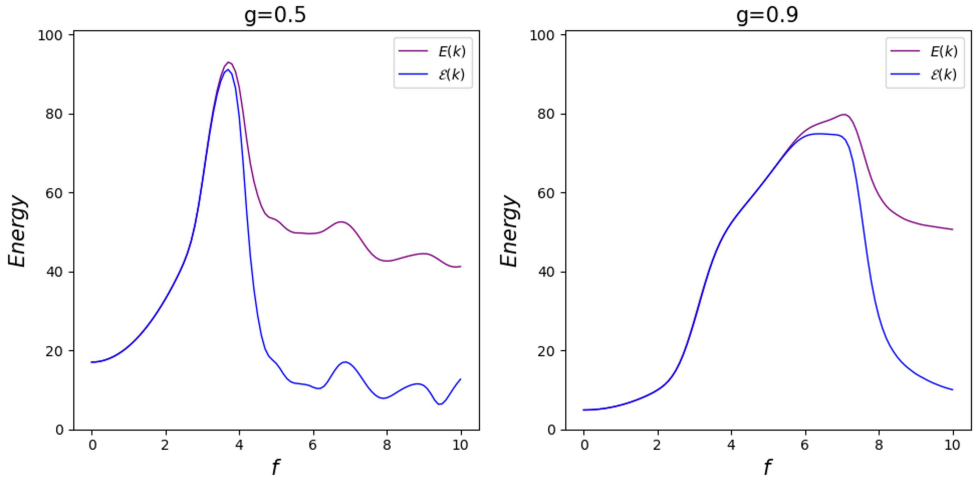

Figure 4. We describe the variation in the energy $E(k)$ and ergotropy $\mathcal{E}_B(k)$ with strength f; the solid purple line represents $E(k)$ and the solid blue line represents $\mathcal{E}_B(k)$.

5. Optical Parametric Amplifier

An optical parametric amplifier (OPA) is an optical device based on the parametric oscillation effect. It utilizes materials such as nonlinear optical crystals to generate a nonlinear coupling effect between photons, thereby achieving amplification of optical signals. An OPA can be used to enhance the intensity of laser beams in optical microscopes, thereby improving the resolution and clarity of images. An OPA has a wider-gain bandwidth and

higher optical performance, and it can be used to increase the power of signal light in fiber optic communication, thereby expanding the transmission distance.

Recently, it has been shown that upon including an OPA inside the cavity, interesting phenomena will occur. An OPA utilizes nonlinear optical effects to amplify the optical field signal input into the cavity. In quantum batteries, it helps to enhance the intensity of the light field interacting with qubits, thereby improving energy transfer efficiency. An OPA can adjust the photon number distribution of the cavity field, thereby optimizing the energy transfer between qubits and the cavity field, and achieving a more efficient energy transfer process. From the above description, we can see that an OPA is a great device, and we are trying to apply it to quantum batteries. In this section, we focus on discussing the impact of adding an OPA to the cavity of the original system model on battery charging.

If we insert an OPA into the cavity of the original battery model, as shown in Figure 5, the Hamiltonian of the system can be expressed as

$$H_O = g(a\sigma_+ + a^\dagger\sigma_-) + iG(e^{i\theta}a^\dagger a^\dagger - e^{-i\theta}aa), \tag{13}$$

where the parameter G represents the nonlinear gain of the OPA, θ represents the phase of the field driving the OPA, and the latter term in the above equation represents the coupling between the cavity and the OPA.

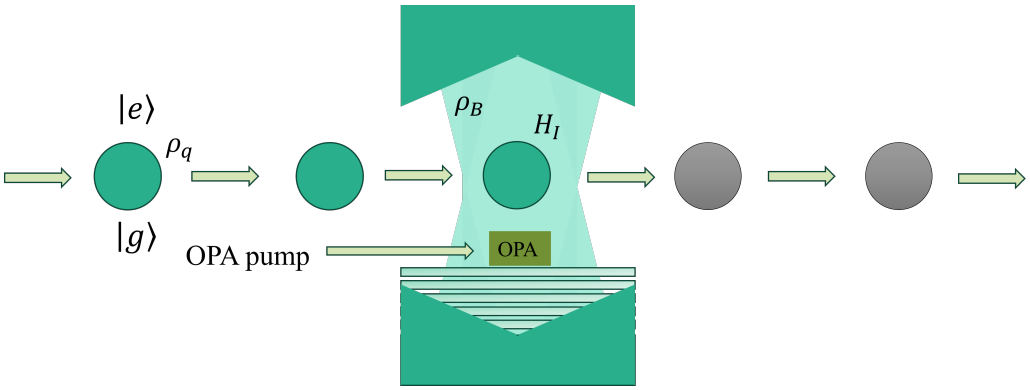

Figure 5. A diagram of a micromaser quantum battery operating via an optical parametric amplifier. We put an OPA in the cavity.

In all the calculations, we truncate the sizes of our Fock space by limiting the bosonic particles associated with the quantum oscillators to 100. Figure 6 shows the results of the numerical simulation.

To compare our model with the original system model, as shown in Figure 6a–c, after multiple numerical calculations, we found an excellent value. We take the coupling strength $g = 0.5$, nonlinear gain $G = 0.976$, and phase $\theta = 0$ in Figure 6a, and the values on the panel are approximately 84.53 and 17.02 from top to bottom. The purple solid line represents the energy of the battery after adding an OPA to the cavity field, and the green solid line represents the energy of the original system battery. It can be seen from the above figure that adding an OPA to the cavity field can significantly increase the battery's energy storage capacity. The blue solid line in Figure 6b represents the ergotropy $\mathcal{E}_B(k)$ of the battery, and the values on the panel are approximately 84.53 and 78.71 from top to bottom. It can be seen that there is a certain gap between the ergotropy $\mathcal{E}_B(k)$ and the energy $E(k)$, but it is still a high value. Figure 6c shows the release efficiency of useful energy in quantum batteries, and it can be calculated that $R(k) \approx 93\%$.

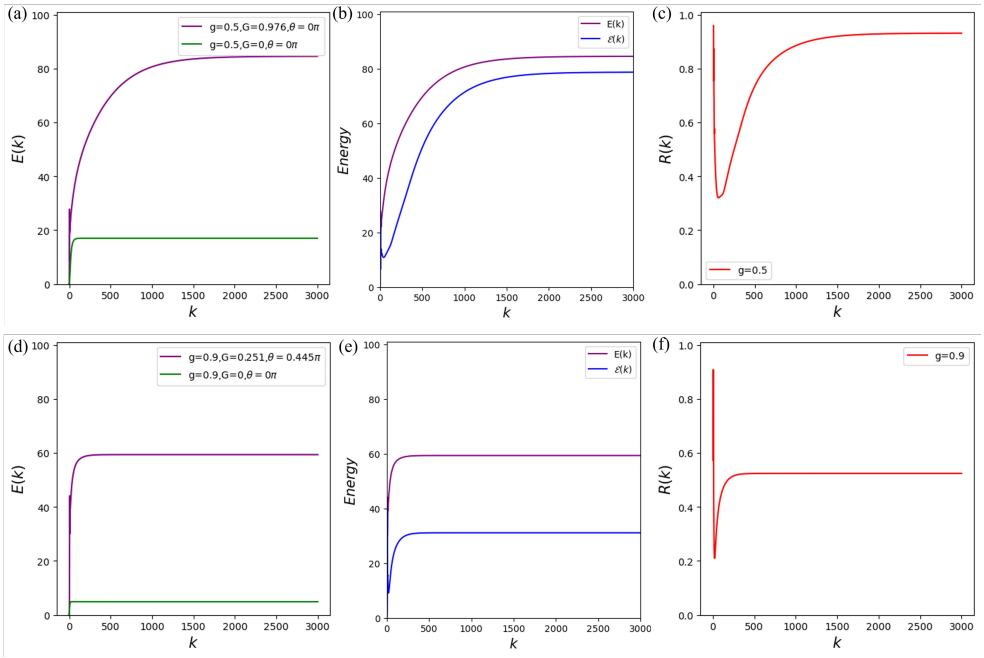

Figure 6. The **left** panel represents the energy stored, the **middle** panel represents the comparison between the energy stored $E(k)$ and ergotropy $\mathcal{E}_B(k)$ of the battery, and the **right** panel represents the efficiency $R(k)$; they are computed for $q = 0.25$. We intercept the Hilbert space $N = 100$. (**a**–**c**) The performance of the micromaser quantum battery when $g = 0.5$; (**d**–**f**) the performance of the micromaser quantum battery when $g = 0.9$.

Below, we discuss the case of coupling strength $g = 0.9$ in Figure 6d–f, with nonlinear gain $G = 0.251$ and phase $\theta = 0.445\pi$. As shown in Figure 6d–f, we can still see from the pictures that the battery with an OPA can store more energy than the battery without an OPA. In Figure 6d, the values on the panel are approximately 59.35 and 4.90 from top to bottom, in Figure 6e, the values on the panel are approximately 59.35 and 31.30 from top to bottom. Although the difference between the extractable energy (ergotropy) $\mathcal{E}_B(k)$ and energy $E(k)$ is somewhat large at this time, overall, it is still better than the original system. After calculation, it can be concluded that the energy release efficiency $R(k) \approx 52\%$.

The above analysis only obtained good values from numerous numerical simulations, proving that adding an OPA can have a good impact on battery charging. Next, we will analyze how the nonlinear gain G and phase θ affect the battery.

Figure 7 shows a thermal map of battery energy with different nonlinear gain G and phase θ values. It can be seen from the figure that the darker the red color, the greater the energy $E(k)$, and conversely, the shallower the red color, the smaller the energy $E(k)$. For the case where the coupling strength $g = 0.5$, it can be clearly seen that as the nonlinear gain G approaches 1 and the phase θ approaches 2π, the energy $E(k)$ increases. However, it can be clearly seen from the graph that when the value of the nonlinear gain G is greater than 1, the effect is not significant in the range of 0 to 1. However, for a coupling strength of $g = 0.9$, as the nonlinear gain G approaches 1 and the phase θ approaches π, the energy $E(k)$ increases. We can clearly observe that regardless of the coupling strength, $g = 0.5$ or $g = 0.9$, the above graph shows a periodic distribution. In summary, we found that adding an OPA to the cavity can improve the performance of the battery to a certain extent.

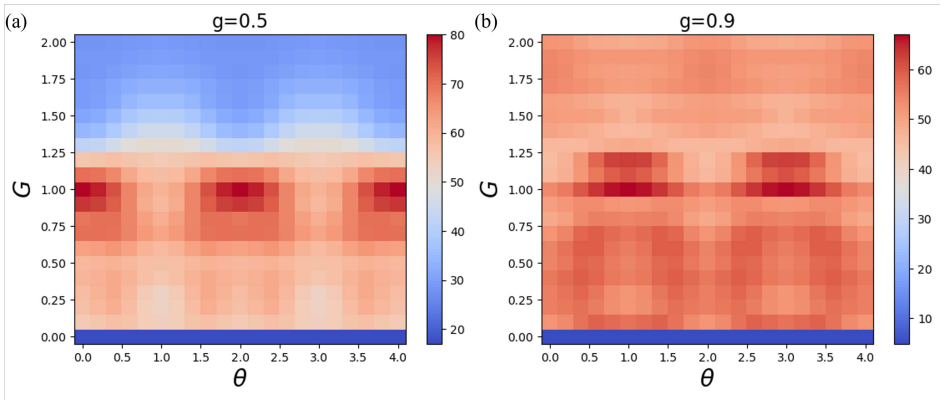

Figure 7. The thermal map of battery energy $E(k)$ when adding an OPA. The horizontal axis of both figures is phase θ, the unit is π, and the vertical axis is nonlinear gain G. We truncate the Hilbert space $N = 100$, and $k = 2000$. (**a**) $g = 0.5$, (**b**) $g = 0.9$.

6. Combining Classic Driving Field and OPA

In the previous two sections, we attempted to add a classical driving field and an OPA to the original system, and found that both can improve the performance of the quantum battery. This makes us wonder what kind of effect would be produced if we combine the two methods. In this section, we discuss how to combine the two and explore the impact of this approach on quantum battery charging.

Classical field driving prepares qubits in specific superposition states or specific phase states, making them more compatible with the amplified optical field generated by an OPA in terms of frequency, phase, and coupling strength. It also enhances the transfer of energy between qubits and cavity fields, and improves the charging speed and energy storage efficiency of quantum batteries. When the OPA-enhanced light field interacts with qubits in a suitable state, it can more effectively exchange energy and information, achieving efficient quantum manipulation and energy transfer.

In Figure 8, we choose the same values as in the previous text, with coupling strength $g = 0.5$, nonlinear gain $G = 0.976$, and phase $\theta = 0$. We find that all three methods can achieve steady state of the quantum battery, which is the result we hope to obtain. And it can be clearly observed that the combined effect is superior to either method, and the extractable energy (ergotropy) $\mathcal{E}_B(k)$ also has a high value, indicating that the combination of these two methods will improve the charging effectiveness of the battery.

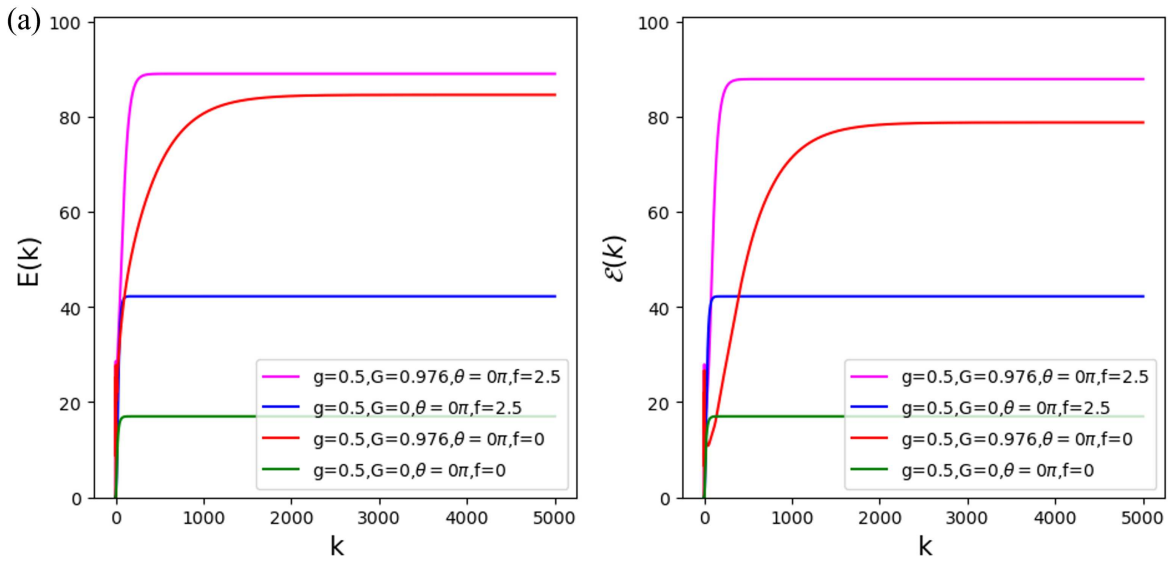

Figure 8. *Cont.*

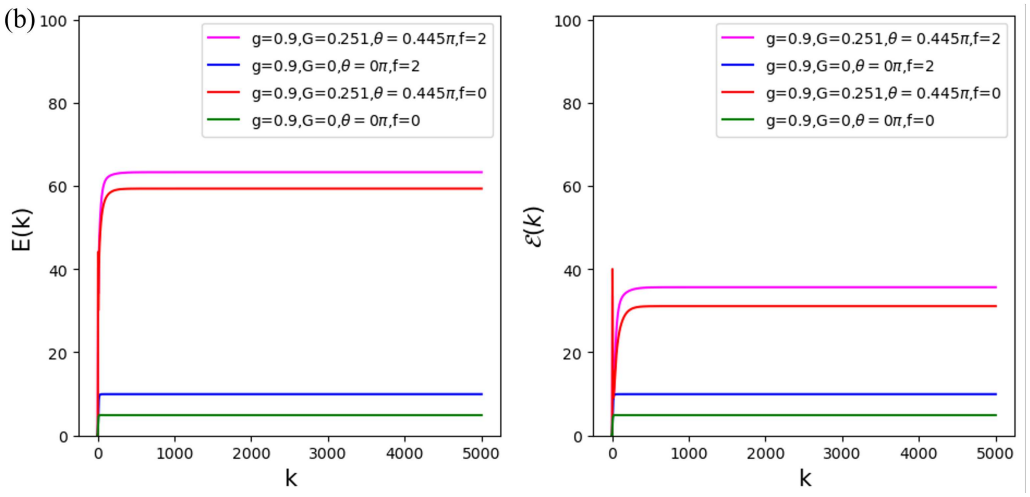

Figure 8. Graphs show the battery's performance when $g = 0.5$ and $g = 0.9$. The **left** panel represents battery energy $E(k)$, and the **right** panel represents ergotropy $\mathcal{E}_B(k)$. The fuchsia solid line represents the situation of combination, the blue solid line represents the situation where only a classical driving field exists, the red solid line represents the situation where only an OPA exists, and the green solid line represents neither of the two. (**a**) The values on the **left** panel are approximately 88.97, 84.54, 42.23, and 17.02 from top to bottom, and those on the **right** panel are approximately 87.86, 78.74, 42.23, and 17.02. (**b**) The values on the **left** panel are approximately 63.39, 59.35, 9.95, and 4.90 from top to bottom, and those on the **right** panel are approximately 35.65, 31.10, 9.95, and 4.90.

For coupling strength $g = 0.9$, nonlinear gain $G = 0.251$, and phase $\theta = 0.445\pi$, it also produces the same effect.

To investigate whether the advantages of this combination method still exist in different initial quantum states of the battery, we set q to 0.8 instead of the original 0.25. It is easy to see from Figure 9 that even if the initial state of the qubit is changed, the advantages of the combination method still exist.

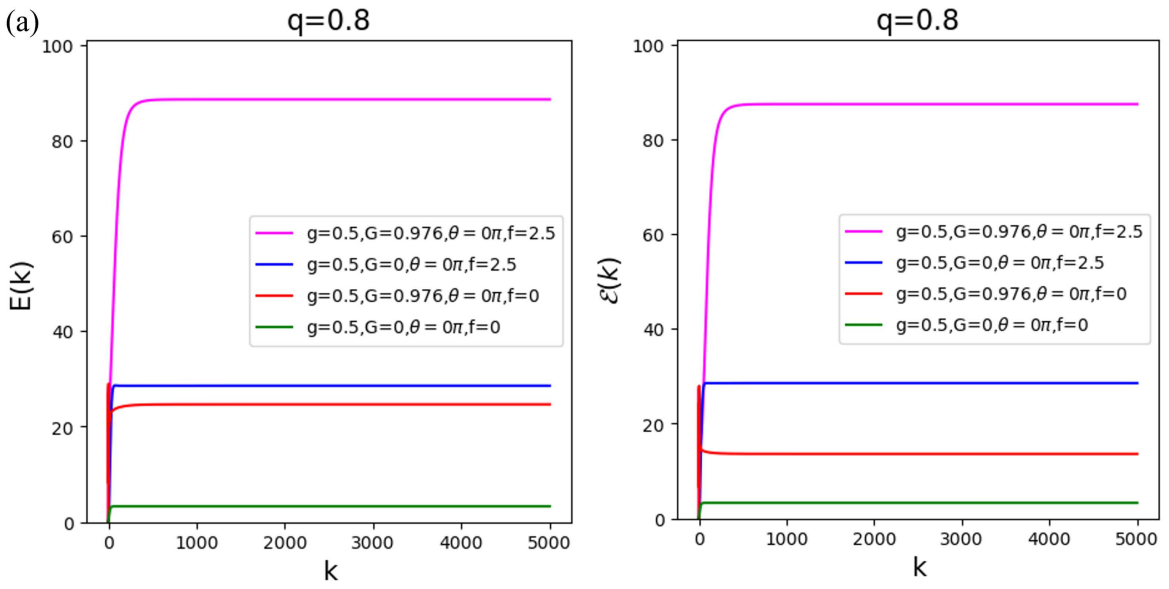

Figure 9. *Cont.*

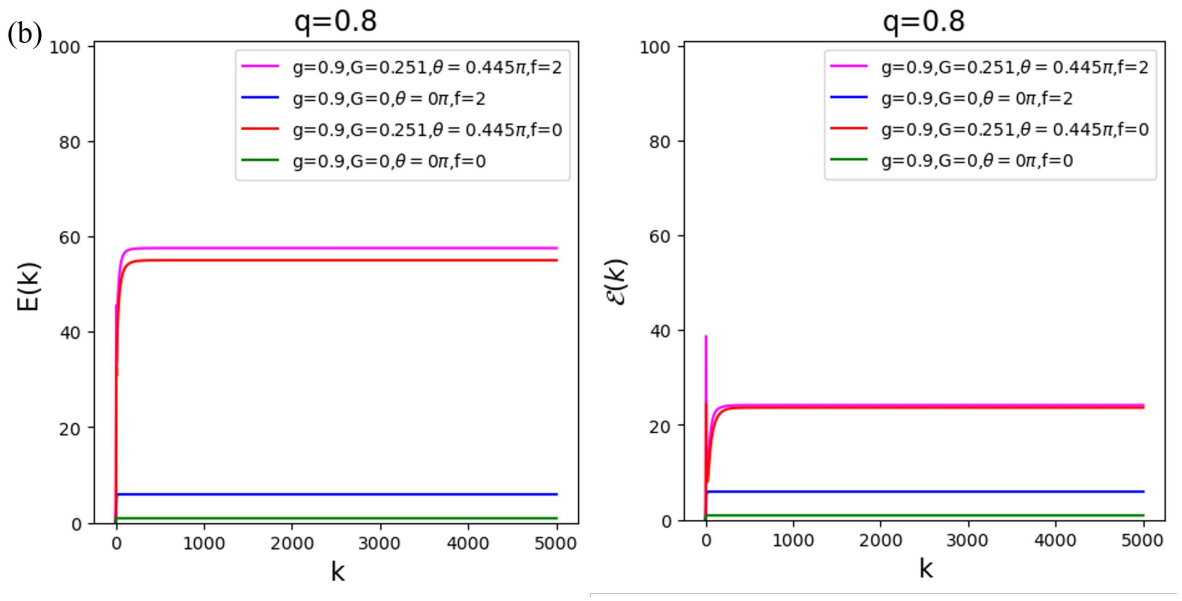

Figure 9. We choose $q = 0.8$, and the other values are the same as in Figure 8. The **left** panel represents the energy stored, and the **right** panel represents the comparison between the energy stored $E(k)$ and ergotropy $\mathcal{E}_B(k)$ of the battery. (**a**) The values on the **left** panel are approximately 88.50, 28.56, 24.65, and 3.30 from top to bottom, and those on the **right** panel are approximately 87.36, 28.55, 13.62, and 3.30. (**b**) The values on the **left** panel are approximately 57.52, 54.97, 5.94, and 0.92 from top to bottom, and those on the **right** panel are approximately 24.18, 23.65, 5.94, and 0.92.

7. Conclusions

In conclusion, in this research on micromaser quantum battery charging, we have performed a rigorous and deep analysis and effectively demonstrated a series of key findings. During the charging process, the use of driving qubits, or the introduction of an OPA in the cavity, or even the organic combination of these two methods, can significantly improve the performance of the battery. Moreover, there are clear and distinct differences in the enhancement effects among these improvement strategies, which can be fully distinguished.

When we use a controlling field to drive qubits, we can clearly observe, through our numerical results, that compared to the original energy increase mode, the energy of this method is slightly improved numerically. It is worth noting that this approach performs excellently in terms of energy utilization efficiency. This is undoubtedly of great significance in the context of efficient energy utilization.

When we place OPA crystals in the cavity, a different scene is presented. The energy has a higher radiation level compared to the original increase, and it can output more powerful energy. However, this approach is not perfect, and in some cases, its energy conversion efficiency may decrease, which also highlights a direction for subsequent optimization research.

When we combine the two methods for charging, we find a good phenomenon whereby both the stored energy and ergotropy are higher than when using any method alone. From the perspective of overall battery performance, these newly constructed battery models demonstrate unparalleled advantages. These new battery models have significant advantages over the original model in terms of the amount of stored energy, charging power, and ergotropy.

We have numerically shown that this model can be considered an excellent model of a quantum battery. Our method retains the characteristic of the original model, maintaining a steady state, which is a good characteristic in quantum batteries. On this basis, the battery's

ability to store and release energy has been improved, making a significant contribution to the study of quantum batteries.

In summary, we think our results show an explicit and promising model of a quantum battery, and we firmly believe that the research results of this study are highly valuable and have successfully demonstrated a clear and promising quantum battery model. This achievement undoubtedly injects a strong driving force into the continuous progress of quantum battery technology, laying a solid foundation for its further development in the future.

Author Contributions: Conceptualization, S.H. and A.C.; methodology, S.H. and A.C.; software, J.Z., S.H. and L.D.; formal analysis, J.Z., S.H. and L.D.; writing—original draft preparation, J.Z., S.H. and L.D.; writing—review and editing, S.H. and A.C. All authors have read and agreed to the published version of the manuscript.

Funding: This research was funded by the National Natural Science Foundation of China (grant numbers 12174344 and 12175199), and by the Foundation of the Department of Science and Technology of Zhejiang Province (grant number 2022R52047).

Institutional Review Board Statement: Not applicable.

Informed Consent Statement: Not applicable.

Data Availability Statement: The data are contained within the article.

Conflicts of Interest: The authors declare no conflicts of interest.

References

1. Barra, F. Dissipative Charging of a Quantum Battery. *Phys. Rev. Lett.* **2019**, *122*, 210601. [CrossRef] [PubMed]
2. Bhattacharjee, S.; Dutta, A. Quantum thermal machines and batteries. *Eur. Phys. J. Condens. Matter Complex Syst.* **2021**, *94*, 239. [CrossRef]
3. Mayo, F.; Roncaglia, A. Collective effects and quantum coherence in dissipative charging of quantum batteries. *Phys. Rev. A* **2022**, *105*, 062203. [CrossRef]
4. Alicki, R.; Fannes, M. Entanglement boost for extractable work from ensembles of quantum batteries. *Phys. Rev. E* **2013**, *87*, 042123. [CrossRef]
5. Andolina, G.M.; Farina, D.; Mari, A.; Pellegrini, V.; Giovannetti, V.; Polini, M. Charger-mediated energy transfer in exactly-solvable models for quantum batteries. *Phys. Rev. B* **2018**, *98*, 205423. [CrossRef]
6. Zhang, Y.Y.; Yang, T.R.; Fu, L.; Wang, X. Powerful harmonic charging in a quantum battery. *Phys. Rev. E* **2019**, *99*, 052106. [CrossRef]
7. Chen, Y.; Hasegawa, Y. Indefinite Causal Order in Quantum Batteries. *arXiv* **2021**, arXiv:2105.12466.
8. Sassetti, M. Characterization of a Two-Photon Quantum Battery: Initial Conditions, Stability and Work Extraction. *Entropy* **2021**, *23*, 612. [CrossRef] [PubMed]
9. Crescente, A.; Carrega, M.; Sassetti, M.; Ferraro, D. Charging and energy fluctuations of a driven quantum battery. *New J. Phys.* **2020**, *22*, 063057. [CrossRef]
10. Le, T.P.; Levinsen, J.; Modi, K.; Parish, M.M.; Pollock, F.A. Spin-chain model of a many-body quantum battery. *Phys. Rev. A* **2018**, *97*, 022106. [CrossRef]
11. Andolina, G.M.; Keck, M.; Mari, A.; Giovannetti, V.; Polini, M. Quantum versus classical many-body batteries. *Phys. Rev.* **2019**, *99*, 205437. [CrossRef]
12. Ghosh, S.; Chanda, T.; Sen, A. Enhancement in the performance of a quantum battery by ordered and disordered interactions. *Am. Phys. Soc.* **2020**, *101*, 032115. [CrossRef]
13. Liu, J.X.; Shi, H.L.; Shi, Y.H.; Wang, X.H.; Yang, W.L. Entanglement and work extraction in the central-spin quantum battery. *Phys. Rev. B* **2021**, *104*, 245418. [CrossRef]
14. Arjmandi, M.B.; Mohammadi, H.; Santos, A.C. Enhancing self-discharging process with disordered quantum batteries. *J. Quantum Stud.* **2021**, *10*, 10–20. [CrossRef]
15. Barra, F.; Hovhannisyan, K.V.; Imparato, A. Quantum batteries at the verge of a phase transition. *New J. Phys.* **2022**, *24*, 015223. [CrossRef]

16. Crescente, A.; Carrega, M.; Sassetti, M.; Ferraro, D. Ultrafast charging in a two-photon Dicke quantum battery. *Phys. Rev. B* **2020**, *102*, 245407. [CrossRef]
17. Huangfu, Y.; Jing, J. High-capacity and high-power collective charging with spin chargers. *Phys. Rev. E* **2021**, *104*, 024129. [CrossRef] [PubMed]
18. Qi, S.F.; Jing, J. Magnon-mediated quantum battery under systematic errors. *Phys. Rev. A* **2021**, *104*, 032606. [CrossRef]
19. Seah, S.; Perarnau-Llobet, M.; Haack, G.; Brunner, N.; Nimmrichter, S. Quantum speed-up in collisional battery charging. *Phys. Rev. Lett.* **2021**, *127*, 100601. [CrossRef] [PubMed]
20. Julià-Farré, S.; Salamon, T.; Riera, A.; Bera, M.N.; Lewenstein, M. Bounds on the capacity and power of quantum batteries. *Phys. Rev. Res.* **2020**, *2*, 023113. [CrossRef]
21. Rossini, D.; Andolina, G.M.; Rosa, D.; Carrega, M.; Polini, M. Quantum Advantage in the Charging Process of Sachdev-Ye-Kitaev Batteries. *Phys. Rev. Lett.* **2020**, *125*, 236402. [CrossRef] [PubMed]
22. Agarwal, S.; Rafsanjani, S.M.H.; Eberly, J.H. Tavis-Cummings model beyond the rotating wave approximation: Quasidegenerate qubits. *Phys. Rev. A* **2012**, *85*, 124–130. [CrossRef]
23. Zhou, L.; Wang, L.; You, L. Optimal state for Tavis-Cummings quantum battery via Bethe ansatz method. *Phys. Rev. A* **2022**, *106*, 012417. [CrossRef]
24. Li, H.; Zhang, K.; Wu, C.; Yang, L.; Shen, H. Reinforcement learning optimization of the charging of a Dicke quantum battery. *Phys. Rev. A* **2022**, *106*, 062416. [CrossRef]
25. Caravelli, F.; Wit, C.D.; García-Pintos, L.P.; Hamma, A. Random quantum batteries. *Phys. Rev. Res.* **2020**, *2*, 023095. [CrossRef]
26. Yao, Y.; Shao, X.Q. Optimal charging of open spin-chain quantum batteries via homodyne-based feedback control. *Phys. Rev. E* **2022**, *106*, 014138. [CrossRef]
27. Salvia, R.; Perarnau-Llobet, M.; Haack, G.; Brunner, N.; Nimmrichter, S. Quantum advantage in charging cavity and spin batteries by repeated interactions. *Phys. Rev. Res.* **2022**, *5*, 013155. [CrossRef]
28. Benenti, G.; Casati, G.; Strini, G. *Principles of Quantum Computation and Information*; World Scientific: Hackensack, NJ, USA, 2004.
29. Quantum supremacy using a programmable superconducting processor. *Nature* **2019**, *574*, 505–510. [CrossRef]
30. Binder, F.; Correa, L.A.; Gogolin, C.; Anders, J.; Adesso, G. *Thermodynamics in the Quantum Regime Fundamental Aspects and New Directions: Fundamental Aspects and New Directions*; Springer: Berlin/Heidelberg, Germany, 2018.
31. Vinjanampathy, S.; Anders, J. Quantum thermodynamics. *Contemp. Phys.* **2016**, *57*, 545–579. [CrossRef]
32. Daryanoosh, S.; Gilchrist, A.; Baragiola, B.Q. Collisional-model quantum trajectories for entangled qubit environments. *Phys. Rev. A* **2022**, *106*, 022202. [CrossRef]
33. Horowitz, J.M. Quantum-trajectory approach to the stochastic thermodynamics of a forced harmonic oscillator. *Phys. Rev. E—Stat. Nonlinear Soft Matter Phys.* **2012**, *85*, 729–734. [CrossRef]
34. Strasberg, P.; Schaller, G.; Brandes, T.; Esposito, M. Quantum and Information Thermodynamics: A Unifying Framework Based on Repeated Interactions. *Phys. Rev. X* **2017**, *7*, 021003. [CrossRef]
35. Landi, G.T. Battery Charging in Collision Models with Bayesian Risk Strategies. *Entropy* **2021**, *23*, 1627. [CrossRef] [PubMed]
36. Jaynes, E.T.; Cummings, F.W. Comparison of Quantum and Semiclassical Radiation Theories with Application to the Beam Maser. *Proc. IEEE* **1963**, *51*, 89–109. [CrossRef]
37. Filipowicz, P.; Javanainen, J.; Meystre, P. Quantum and semiclassical steady states of a kicked cavity mode. *J. Opt. Soc. Am. B* **1986**, *3*, 906–910. [CrossRef]
38. Slosser, J.J.; Meystre, P.; Braunstein, S.L. Harmonic oscillator driven by a quantum current. *Phys. Rev. Lett.* **1989**, *63*, 934. [CrossRef] [PubMed]
39. Slosser, J.J.; Meystre, P.; Wright, E.M. Generation of macroscopic superpositions in a micromaser. *Opt. Lett.* **1990**, *15*, 233. [CrossRef] [PubMed]
40. Shaghaghi, V.; Singh, V.; Benenti, G.; Rosa, D. Micromasers as quantum batteries. *Quantum Sci. Technol.* **2022**, *7*, 04LT01. [CrossRef]
41. Shaghaghi, V.; Singh, V.; Carrega, M.; Rosa, D.; Benenti, G. Lossy Micromaser Battery: Almost Pure States in the Jaynes—Cummings Regime. *Entropy* **2023**, *25*, 430. [CrossRef] [PubMed]
42. Huang, B.; Li, C.; Fan, B.; Duan, Z. Dissipation-Induced Photon Blockade in the Anti-Jaynes—Cummings Model. *Photonics* **2024**, *11*, 369. [CrossRef]
43. Huang, J.F.; Liao, J.Q.; Kuang, L.M. Ultrastrong Jaynes-Cummings model. *Am. Phys. Soc.* **2020**, *101*, 043835. [CrossRef]
44. Friis, N.; Huber, M. Precision and Work Fluctuations in Gaussian Battery Charging. *Quantum* **2018**, *2*, 61. [CrossRef]
45. Chung, D.D.L. Electromagnetic interference shielding effectiveness of carbon materials. *Carbon* **2001**, *39*, 279–285. [CrossRef]
46. Leggett, A.J. Qubits, Cbits, Decoherence, Quantum Measurement and Environment. In *Fundamentals of Quantum Information: Quantum Computation, Communication, Decoherence and All That*; Springer: Berlin/Heidelberg, Germany, 2002.
47. Yang, X.; Yang, Y.H.; Alimuddin, M.; Salvia, R.; Fei, S.M.; Zhao, L.M.; Nimmrichter, S.; Luo, M.X. Battery Capacity of Energy-Storing Quantum Systems. *Phys. Rev. Lett.* **2023**, *131*, 030402. [CrossRef]

48. Hovhannisyan, K.V.; Perarnau-Llobet, M.; Huber, M.; Acin, A. Entanglement Generation is Not Necessary for Optimal Work Extraction. *Phys. Rev. Lett.* **2013**, *111*, 240401. [CrossRef]
49. Andolina, G.M.; Keck, M.; Mari, A.; Campisi, M.; Polini, M. Extractable work, the role of correlations, and asymptotic freedom in quantum batteries. *Phys. Rev. Lett.* **2019**, *122*, 047702. [CrossRef] [PubMed]
50. Yang, R.G.; Li, N.; Zhang, J.; Li, J.; Zhang, T.C. Enhanced entanglement of two optical modes in optomechanical systems via an optical parametric amplifier. *J. Phys. At. Mol. Phys.* **2017**, *50*, 085502. [CrossRef]
51. Lü, X.Y.; Wu, Y.; Johansson, J.R.; Jing, H.; Zhang, J.; Nori, F. Squeezed Optomechanics with Phase-Matched Amplification and Dissipation. *Phys. Rev. Lett.* **2015**, *114*, 093602. [CrossRef] [PubMed]
52. Li, L.; Nie, W.; Chen, A. Transparency and tunable slow and fast light in a nonlinear optomechanical cavity. *Sci. Rep.* **2016**, *6*, 35090. [CrossRef] [PubMed]
53. Quach, J.Q.; Munro, W.J. Using dark states to charge and stabilise open quantum batteries. *Phys. Rev. Appl.* **2020**, *14*, 024092. [CrossRef]
54. Binder, F.C.; Vinjanampathy, S.; Modi, K.; Goold, J. Quantacell: Powerful charging of quantum batteries. *New J. Phys.* **2015**, *17*, 075015. [CrossRef]
55. Campaioli, F.; Pollock, F.A.; Binder, F.C.; Celeri, L.; Goold, J.; Vinjanampathy, S.; Modi, K. Enhancing the Charging Power of Quantum Batteries. *Phys. Rev. Lett.* **2017**, *118*, 150601. [CrossRef]
56. Ferraro, D.; Campisi, M.; Andolina, G.M.; Pellegrini, V.; Polini, M. High-Power Collective Charging of a Solid-State Quantum Battery. *Phys. Rev. Lett.* **2018**, *120*, 117702. [CrossRef]
57. García-Pintos, L.P.; Hamma, A.; Campo, A.D. Fluctuations in Extractable Work Bound the Charging Power of Quantum Batteries. *Phys. Rev. Lett.* **2020**, *125*, 040601. [CrossRef]
58. Allahverdyan, A.E.; Balian, R.; Tim, N. Maximal work extraction from finite quantum systems. *Europhys. Lett.* **2004**, *67*, 565. [CrossRef]
59. Liu, Y.; Ren, X.; Zhou, X.; Lan, D.; Gao, Z.; Jia, Z.; Wu, G. Defect design and vacancy engineering of $NiCo_2Se_4$ spinel composite for excellent electromagnetic wave absorption. *Ceram. Int.* **2024**, *50*, 46643–46652. [CrossRef]
60. Zheng, J.; Lan, D.; Zhang, S.; Wei, F.; Liu, T.; Gao, Z.; Wu, G. Zeolite imidazolate framework derived efficient absorbers: From morphology modulation to component regulation. *J. Alloys Compd.* **2025**, *1010*, 177092. [CrossRef]
61. Li, R.; Li, J.; Liu, Q.; Li, T.; Lan, D.; Ma, Y. Recent progress on covalent organic frameworks and their composites as electrode materials for supercapacitors. *Adv. Compos. Hybrid Mater.* **2025**, *8*, 86. [CrossRef]
62. Niu, Z.; Wang, Y.; Tian, Q.; Wang, J.; Gao, Z.; Lan, D.; Wu, G. Hierarchical aggregation structure regulation and electromagnetic loss mechanism of cross-linked polyaniline in polymer wave absorbers. *Carbon* **2025**, *233*, 119848. [CrossRef]
63. Xue, R.; Lan, D.; Qiang, R.; Zang, Z.; Ren, J.; Shao, Y.; Rong, L.; Gu, J.; Fang, J.; Wu, G. Synergistic dielectric regulation strategy of one-dimensional $MoO_2/Mo_2C/C$ heterogeneous nanowires for electromagnetic wave absorption. *Carbon* **2025**, *233*, 119877. [CrossRef]
64. Xie, X.; Liu, R.; Chen, C.; Lan, D.; Chen, Z.; Du, W.; Wu, G. Phase changes and electromagnetic wave absorption performance of XZnC (X = Fe/Co/Cu) loaded on melamine sponge hollow carbon composites. *Int. J. Miner. Metall. Mater.* **2024**, *32*, 566. [CrossRef]
65. Mu, Z.; Sun, Y.; Qin, J.; Shen, Z.; Liang, G.; Zou, J.; Lan, D.; Xie, P. Flexible carbon nanocomposite fabric with negative permittivity property prepared by electrostatic spinning. *Adv. Compos. Hybrid Mater.* **2025**, *8*, 77. [CrossRef]
66. Johansson, J.R.; Nation, P.D.; Nori, F. QuTiP 2: A Python framework for the dynamics of open quantum systems. *Comput. Phys. Commun.* **2013**, *184*, 1234–1240. [CrossRef]